HiSST: 3rd International Conference on
High-Speed Vehicle Science Technology
14 -19 April 2024, Busan, Korea

Comparative Analysis of Rectangular-to-Elliptical Shape Transition (REST) intakes with Diverse Leading-Edge Profiles

Daegi Yeom[1], Hyeonseo Lee[2], Seongkyun Im[3]

Abstract

The on- and off-design performances of three rectangular-to-elliptical shape transition (REST) with diverse leading-edge profiles were examined numerically. In the design and analysis of REST intakes, particular attention was given to the notching process, a critical post-processing step that significantly influences the overall flow characteristics and performance of these intakes. The designated Mach number (Ma) for the study was fixed at 7, and all intakes were designed with an approximately 10 contraction ratio (CR), a uniform truncation angle of 3°, and a notching percentage of 2%. The first intake, denoted as Type A, was characterized by a leading-edge shaped according to a sinusoidal function. In contrast, the second and third intakes employed quadratic functions for leading-edge shaping, with convex and concave fitting lines, respectively. Computational fluid dynamics (CFD) simulations were conducted to assess the performance of each REST intake, with a focus on key parameters including total pressure recovery rate, pressure ratio, inlet exit Ma, and captured mass flow rate. The results of this study indicate that the second type of REST intake exhibited notable advantages in achieving a high degree of compression, despite the restricted starting range to Ma 5. Conversely, the third type of REST intake demonstrated the ability to extend the operational range to a lower starting limit of Ma 4.5. These results shed light on the potential benefits and limitations of various leading-edge profiles in REST intakes, thereby contributing to the advancement of intake design for scramjet propulsion systems.

Keywords : *Scramjet, Streamline tracing inlet, REST, Hypersonic, CFD*

Nomenclature

CR	:	contraction ratio
Ma	:	Mach number
PR	:	pressure ratio
TPR	:	total pressure ratio
M_1	:	design Ma
M_3	:	post-shock Ma
θ_{shock}	:	shock angle
u	:	radial Ma
v	:	azimuthal Ma

1. Introduction

For the efficient design of an intake for a scramjet propulsion system, it is advisable to employ the streamline-tracing method, which leverages the Busemann intake flow field. Within the Busemann flow field, the primary means of compression occurs through area contraction and flow turning, which are regarded as isentropic processes. Consequently, this approach minimizes the impact of flow deflection, which might otherwise lead to total pressure losses and a reduction in thrust. In this study, an intake

[1] *Department of Mechanical Engineering, 145, Anam-ro, Seongbuk-gu, 319 Innovation Hall, Seoul, 02841, Republic of Korea, limbo135@korea.ac.kr*
[2] *Department of Mechanical Engineering, 145, Anam-ro, Seongbuk-gu, 319 Innovation Hall, Seoul, 02841, Republic of Korea, wlsakstns@korea.ac.kr*
[3] *Department of Mechanical Engineering, 145, Anam-ro, Seongbuk-gu, 319 Innovation Hall, Seoul, 02841, Republic of Korea, sim3@korea.ac.kr*

with a rectangular-to-elliptical shape transition (REST), representing one of the morphed Busemann intakes, was created and assessed. In contrast to the conventional approach, the notching process was treated as a distinct post-processing step to evaluate the intake's performance based on variations in the shape of the leading edge. The notching line was determined by tracing the iso-Ma points, considering a predefined notching percentage, along the intake's wall. According to the method of interpolating iso-Ma points, three distinct notching line shapes were derived. Three different REST intakes were subjected to evaluation of their on- and off-design performances using computational fluid dynamics (CFD) simulations.

2. Methodology

2.1. Design method

The design process was initiated by obtaining the Busemann streamlines for the design point. The streamline, serving as the parent flow field, is derived from the Taylor-Maccoll equation [1]. Initial conditions for this process include the Ma of the design point (M_1), the post-termination shock Ma (M_3), the termination shock angle (θ_{shock}), as well as atmospheric pressure, and temperature. Eq. 1 and 2 describe a system of differential equations formulated using radial Ma (u) and azimuthal Ma (v). Each directional Ma is obtained through iterative solutions of these differential equations, subsequently becoming an additional boundary condition as specified in Eq. 3. The iterative integration process continues until the achieved Ma corresponds to the specified value of M_1.

$$\frac{du}{d\theta} = v + \frac{\gamma-1}{2} uv \frac{u+v\cos\theta}{v^2-1} \tag{1}$$

$$\frac{dv}{d\theta} = -u + \left(1 + \frac{\gamma-1}{2} v^2\right) \frac{u+v\cot\theta}{v^2-1} \tag{2}$$

$$\frac{dr}{d\theta} = \frac{ru}{v} \tag{3}$$

The subsequent step involves determining the truncation angle and executing morphing through the utilization of a blending function. In this study, a truncation angle of 3° was chosen taking into account the influence of viscous effects. Furthermore, two intakes, each rectangular and elliptical cross-sectional shapes, were generated through a wavecatching process. Following this, both streamlines were blended using the blending function described in Eq. 4 and 5, with $R(x,\theta)$ representing the streamline associated with the rectangular shape intake, and $E(x,\theta)$ signifying the streamline related to the elliptical shape intake [2].

$$F(x) = x^{\alpha}, \quad \alpha = 5 \tag{4}$$

$$REST(x,\theta) = R(x,\theta) \cdot \big(1 - F(x)\big) + E(x,\theta) \cdot F(x) \tag{5}$$

Lastly, notching with iso-Ma points, derived from inviscid numerical simulation, was carried out as a post-processing. The specifications of three different types of REST intakes, determined using the interpolation method, are outlined in Table 1.

Table 1. Specifications of designed intakes

Type.	Design Ma	Truncation angle (°)	CR	Notching percentage (%)	Interpolation method
A	7	3	10.21	2	Sinusoidal function
B					A convex quadratic function
C			10.3		A concave quadratic function

2.2. Numerical simulation

To assess the performance of the designed intakes, the steady-state Reynolds-Averaged Navier-Stokes (RANS) equations for three-dimensional, compressible flow were solved using a density-based CFD solver within ANSYS Fluent. The advection upstream splitting method (AUSM) with second-order spatial discretization schemes was employed to compute the flux. The viscosity model chosen was the k-omega SST turbulence model [3]. For thermodynamic properties, the NASA 9-coefficient polynomial and Sutherland's law were utilized to calculate c_p and μ, respectively. The grid independency confirmed that employing 7,640,000 tetrahedral cells secures sufficient convergence. Numerical simulations were

conducted for various Ma conditions to evaluate the on- and off-design performances. The key parameters were total pressure recovery (TPR), pressure ratio (PR), intake's exit Ma, and captured mass flow rate.

3. Results

Fig. 2 depicts the distribution of Ma at the design point within the flow entering the inlet. All three intakes exhibit isentropic compression achieved through a combination of area contraction and flow turning. While Type. A and C correctly position the leading-edge shock on the cowl closure, type. B, with its downwardly convex configuration, displays a larger boundary layer and experiences flow separation. It is also confirmed by examining the Ma contours at the outlet of the intake. Only Type. B exhibits flow separation at the bottom, whereas others display a relatively uniform flow field.

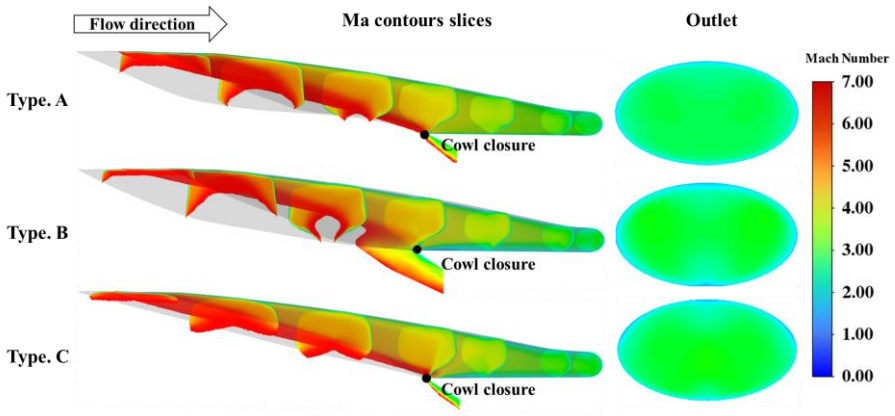

Fig 1. Ma contours at the design point (Ma = 7)

In the off-design conditions, the locations at which the leading-edge shock impacts the intake differ from those in the on-design condition. All three intakes displayed a consistent trend. As the Ma decreases, the shock wave angle increases, causing the leading-edge shock wave to move upstream of the cowl closure. Conversely, when the Ma exceeds the design point Ma, the leading-edge shock wave is swallowed into the intake. The Ma contours at the symmetry plane and outlet for the off-design conditions are presented in Fig. 3.

The results of the performance evaluations for each REST intake are summarized in Table 2. the Type. B intake, characterized by a convex shape notching line, exhibited the most significant compression based on the values of Inlet exit Ma and PR. In terms of efficiency, Type. A intake, featuring a concave shape notching line, achieved the highest level of total pressure recovery. Additionally, only the Type. A intake secured self-starting capability under the predefined starting limit condition, where the Ma is set at 4.5.

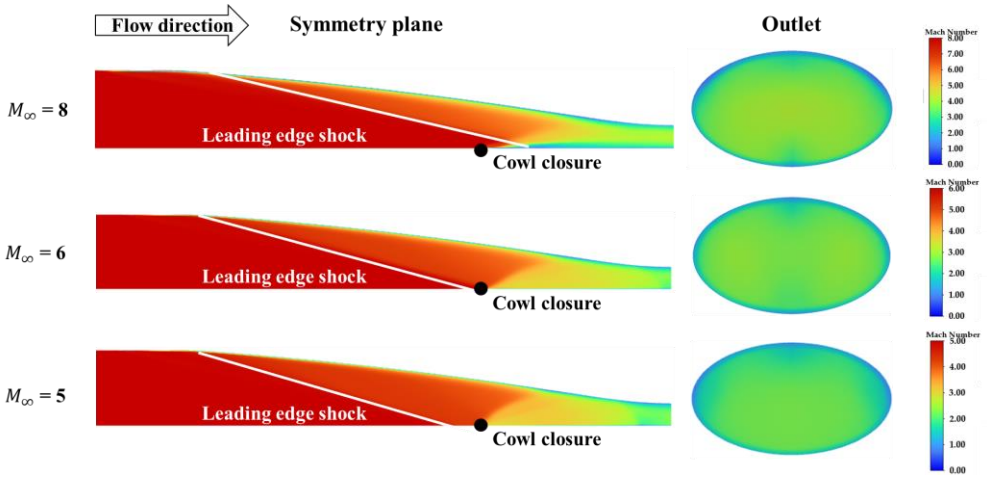

Fig 2. Ma contours at the off-design conditions (Ma = 5, 6, and 8)

Table 2. The performance results of three REST intakes for Ma 5 and 7 conditions

		Type. A	Type. B	Type. C
Ma = 5	Inlet exit Ma	1.99	1.91	2.07
	TPR	0.6465	0.6671	0.6778
	PR	46.21	52.71	41.91
	Mass flow rate (kg/s)	65.57	69.89	60.73
Ma = 7	Inlet exit Ma	3.18	3.14	3.24
	TPR	0.5049	0.5077	0.5402
	PR	47.43	49.03	44.16
	Mass flow rate (kg/s)	44.21	44.08	42.29

4. Conclusion

The shape of the notching line can be tailored by selecting an appropriate interpolation method to trace the iso-Mach points derived from inviscid numerical simulations. Moreover, the design of the REST intake, which fulfills the requirements for both on- and off-design conditions, can be achieved by choosing the configuration of the notching line.

Type A intake, utilizing the sinusoidal function, displayed the lowest TPR rate. This was due to the notching line's complexity, resulting in the generation of a complex shock structure in the internal flow field. In contrast, Type B intake, which employed a convex quadratic interpolation method, achieved the most compression, mainly due to its higher proportion of sidewalls compared to the others. However, the Type C intake exhibited the highest TPR rate and the region where the intake maintained self-starting capability. By removing a substantial portion of sidewalls along the concave quadratic function, Type C intake led to additional mass spillage, which enabled it to avoid choked flow under relatively lower Mach number conditions than the other cases.

Notably, Types B and C showed the most significant performance discrepancy at a Mach number of 5, with differences of 2% in inlet exit Mach number, 7% in TPR, 20% in PR, and 13% in captured mass flow rate. As a result, selecting a concave quadratic function is advantageous when considering the operational range of the scramjet engine, whereas choosing a convex quadratic function is preferable when compression level is a priority.

References

1. Mölder, Sannu. : The busemann air intake for hypersonic speeds. In : Hypersonic Vehicles-Past, Present and Future Developments, pp. 1-38 (2019)
2. Smart, M. K. : Design of three-dimensional hypersonic inlets with rectangular-to-elliptical shape transition. Journal of Propulsion and Power 15.3, 408-416 (1999)
3. Parent, Bernard, and Jean Pascal Sislian. : Validation of the wilcox k-omega model for flows characteristic to hypersonic airbreathing propulsion. AIAA journal 42.2, 261-270 (2004)